Energy Engineering

Tech Science Press

DOI: 10.32604/EE.2021.017464

ARTICLE

Optimal Configuration of an Off-Grid Hybrid Wind-Hydrogen Energy System: Comparison of Two Systems

Zekun Wang[1,2,4], Yan Jia[1,2,3,*], Yingjian Yang[1], Chang Cai[4,5] and Yinpeng Chen[1]

[1]School of Energy and Power Engineering, Inner Mongolia University of Technology, Hohhot, 010051, China
[2]Key Laboratory of Wind Energy and Solar Energy Technology (Inner Mongolia University of Technology), Ministry of Education, Hohhot, 010051, China
[3]Inner Mongolia Autonomous Region Wind Power Technology and Testing Engineering Technology Research Center, Inner Mongolia University of Technology, Hohhot, 010051, China
[4]Institute of Engineering Thermophysics, Chinese Academy of Sciences, Beijing, 100190, China
[5]Key Laboratory of Wind Energy Utilization, Chinese Academy of Sciences, Beijing, 100190, China
*Corresponding Author: Yan Jia. Email: jia-yan@imut.edu.cn

Received: 12 May 2021 Accepted: 28 July 2021

ABSTRACT

Due to the uncertainty of renewable energy power generation and the non-linearity of load demand, it becomes complicated to determine the capacity of each device in hybrid renewable energy power generation systems. This work aims to optimize the capacity of two types of the off-grid hybrid wind-hydrogen energy system. We considered the maximum profit of the system and the minimum loss of power supply probability as optimization goals. Firstly, we established steady-state models of the wind turbine, alkaline electrolyzer, lead-acid battery, and proton exchange membrane fuel cell in matrix laboratory software to optimize the capacity. Secondly, we analyzed the operating mode of the system and determined two system structures (system contains batteries whether or not). Finally, according to the wind speed and load in the sample area, we compared the economics of the two systems and selected the optimal configuration for the area. In the same calculation example data, the non-dominated sorting genetic algorithm-II (NSGA-II) is used to optimize the capacity of each device in the two systems. The results showed that the profit of the without battery-equipped system is 32.38% higher than another system. But the power supply reliability is the opposite. To avoid the contingency of the calculation results, we used the traditional genetic algorithm (GA) and ant colony optimization (ACO) to calculate the same example. The results showed that NSGA-II is significantly better than GA and ACO in terms of iteration steps and calculation results. The required architecture for the System-I composes of 3 numbers of 10 kW wind turbines, 61 sets of 12 V·240 Ah lead-acid batteries, 8 kW electrolytic cell, and 6 kW PEMFC. The net profit and LPSP are ¥44,315 and 0.01254 respectively. The required architecture for the System-II composes of 2 numbers of 10 kW wind turbines, 24 kW electrolytic cells, and 18 kW PEMFC. Net profit and LPSP are ¥58,663 and 0.03244, respectively. This paper provided two schemes for the optimal configuration of the hybrid wind-hydrogen energy system in islanding mode, which provided a theoretical basis for practical engineering applications.

KEYWORDS

Optimization; wind energy; hybrid energy system; off-grid; fuel cell

Nomenclature

DC	Direct current
Q_{tank}	Volume of the hydrogen storage tank
AC	Alternating current
$Q_{AE,T}$	Hydrogen produced by electrolyzer during T period
v_{rated}	Rated wind speed of wind turbine
$Q_{FC,T}$	Hydrogen consumption of PEMFC during T period
$v(t)$	Wind speed at time t
η_t	Efficiency of storing hydrogen
v_{in}	Cut in wind speed
η_{PEM}	Conversion efficiency of PEMFC
v_{out}	Cut out wind speed
η_{AE}	Electrolysis efficiency of alkaline electrolyzer
v_W	Wind speed at the height of the wind turbine hub
N_{AE}	Capacity of the alkaline electrolyzer
v_H	Wind speed measured at height H_H
N_{hst}	Actual hydrogen storage
$P_W(t)$	Power output of wind turbine at time t
R_{net}	Net profit of the system
$P_{bat-c}(t)$	Charging power of the battery at time t
$R_{H_2,T}$	Annual sales revenue of hydrogen during T period
$P_{bat-in}(t)$	Input power of the battery at time t
R_{EN}	Environmental benefits during T period
$P_{bat-f}(t)$	Discharging power of the battery at time t
C_0	Average annual cost
$P_{bat-out}(t)$	Output power of the battery at time t
C_N	Hydrogen storage tank capacity per unit
P_{AE}	Rated power of alkaline electrolyzer
C_T	Cost of the whole life cycle
P_{net}	Net power of the system
C_C	Cost of initial purchase
P_{ex}	Excess electricity in the system
C_M	Cost of operation and maintenance
P_{PEM}	Output power of PEMFC
C_R	Cost of replacement
P_0	Rated power of wind turbine
R_{net}	Net profit of the system
P_{BN}	Rated power of the battery
S_{H_2}	Selling price of hydrogen
P_{FN}	Rated power of PEMFC
V_N	Output voltage of alkaline electrolyzer
$P_L(t)$	Load demand power at time t
H_W	The height of the wind turbine hub
Q	Hydrogen volume
N_A	Avogadro constant
Q_{net}	Net energy accumulation
$SOC_{\max}$	Maximum SOC of the battery
Q_t	Equivalent chemical energy of Q volume hydrogen
$SOC_{\min}$	Minimum SOC of the battery
Q_{in}	Amount of hydrogen input

i	Annual interest rate
Q_N	Rated hydrogen production rate of alkaline electrolyzer
r_0	Hydrogen compression ratio
Q_0	Rated capacity of the battery
y	Life of the equipment

1 Introduction

In recent years, people have developed a strong interest in the application of renewable energy. The main reason is that the traditional fossil energy reserves are limited, and the energy market is unstable [1,2]. On the other hand, it is due to the increasing environmental pollution [3]. Moreover, the unlimited nature of renewable energy is very beneficial to future energy development.

At present, it is urgent to solve the problem of energy waste caused by the long-distance transmission of electricity to remote areas [4]. It is also showed the importance of off-grid renewable energy power generation systems. Wind energy, due to its low pollution and cost, is currently one of the main ways to change the world's environment and energy problems [5,6]. It is of great significance to improving the global energy structure and reducing electricity costs. Nowadays, people have paid great attention to the construction of hybrid renewable energy power generation systems [7–9].

However, the shortcomings of wind power generation such as power fluctuation and output intermittent, have also emerged [10]. The hydrogen storage system has the characteristics of fast charging (discharging) and large capacity [11–13]. It is used in conjunction with wind turbines to effectively solve the fluctuation and intermittent problems of wind power generation. What is more, it can improve the reliability and safety of the system power supply. The hybrid energy system composed of electrolyzer and batteries or fuel cells has complementary advantages [14]. It is used to smooth the volatility of the output power and has technical and economic benefits. It is worth noting that the capacity of the storage system will affect the cost of the power generation system [15]. Therefore, the economic optimization of off-grid renewable energy power generation systems has become a research focus. Wu et al. [16] used the hybrid iteration-adaptive hybrid genetic algorithm (HIAGA) to calculate the objective function of life cycle-net present cost (NPC). They calculated the optimal capacity ratio between wind turbines, photovoltaic (PV) arrays, and battery installations. In [17], Chen et al. used an adaptive genetic algorithm (AGA) to optimize the installation capacity of a stand-alone hybrid wind-solar generation system. In [18], they used the hybrid optimization model for electric renewables (HOMER) software to do the simulations and perform the techno-economic evaluation for a standalone hybrid solar-wind system with battery energy storage for a remote island. It is the early hybrid renewable energy power generation system (hybrid wind-solar generation system). Subsequently, more and more scholars try to add other energy sources to the power generation unit. In [19], they used the genetic algorithm to optimizing and analyzing a stand-alone PV-wind-battery-diesel hybrid system to meet the electricity needs of Fanisua. Li et al. [20] modelled and optimized in HOMER for different combinations of PV panels, wind turbine, and biogas generator. In [21], they used the flower pollination algorithm to optimize the configuration of off-grid solar photovoltaic fuel cell (PV/FC) hybrid systems. Moreover, they compared with the artificial bee colony algorithm and the particle swarm optimization. The advantage of solar power generation is that it can compensate for the intermittent nature of wind power generation. However, as mentioned in [22], solar power still harms the environment. In recent years, the cost of solar power generation has declined [23],

but solar energy is still in the ranks of high-cost energy. Also, the safe operation of solar power generation needs to be improved. Therefore, this paper is aimed at hybrid energy systems operated in islanding mode and did not consider added solar power generation.

The improvement of energy storage systems has also become one of the research hotspots. In [24], they took two types of electrochemical batteries (Lithium Nickel Manganese Cobalt Oxide; and PbO_2-Lead-Acid Battery) into a hybrid generation system for energy storage. In [25], they considered three different battery technologies in hybrid generation system, including Flooded Lead Acid (FLA), Lithium Ferro Phosphate (LFP), and Nickel Iron (Ni–Fe). Nowadays, more and more scholars pay attention to the advantages of high utilization rate and convenient storage of hydrogen energy storage. References [26–28] used an electrolyzer and hydrogen storage tank in a hybrid renewable energy power generation system to store excess electricity. The fuel cell consumed hydrogen energy to generate electricity when the output power of the power generation unit cannot meet the power demand of the load.

At present, scholars from all over the world have optimized the hybrid energy system in different research directions. As far as the economic optimization of the system is concerned, the goal is to minimize the total cost of system operation or maximize the profit based on meeting the load demand [29,30]. But for a region that has never established an integrated energy system, we need to determine which system is suitable for the region through simulation calculations. Therefore, we need to compare the economics of different systems when other conditions are the same. Through the comparative analysis of the results, we can provide options for future system construction. This is also the significance of this study.

This work aims to optimize the capacity of the two kinds of hybrid wind-hydrogen energy (HWHE) system in islanding mode, considered the maximum profit of the system and the minimum loss of power supply probability. Firstly, we established steady-state models of the wind turbine, alkaline electrolyzer, lead-acid battery and proton exchange membrane fuel cell in matrix laboratory software to optimize the capacity. Secondly, we analyzed the operating mode of the system and determined two system structures (the system contains batteries whether or not). Finally, according to the wind speed and load data in the calculation example area, the annual power generation of the system is estimated with the loss of power supply probability as the constraint condition. In the same calculation example data, the non-dominated sorting genetic algorithm-II (NSGA-II), genetic algorithm (GA) and ant colony optimization (ACO) is used to optimize the capacity of each device in the two systems.

The contribution of this study is as follows: i) Because of the optimization of a single system in the current research, this paper used two systems for comparison. ii) Through the analysis of the calculation results and calculation speed of NSGA-II, GA, and ACO, NSGA-II has shown good adaptability in the optimization of the HWHE system. iii) To compare the final optimization results, we analyzed the advantages and disadvantages of the two systems. It provided a reference for actual construction in the future. This study is organized as follows. Section 2 introduced the structure of the HWHE system and the mathematical model of the main components. Section 3 introduced the optimized algorithm and economic modeling. In the fourth section, a case study in Northwest China is simulated and verified. Section 5 summarized the conclusion.

2 Description of the HWHE System

In this section, we introduced the structure of two kinds of wind-hydrogen hybrid energy systems. Besides, we established mathematical models of the main components.

2.1 Structure of the HWHE System

In this paper, we proposed two kinds of HWHE systems (System I & System II). The common feature of the two system structures is that they both contain a wind turbine, alkaline electrolyzer, hydrogen storage tank, PEMFC, inverter and rectifier. The difference is that System I contain lead-acid batteries. The structure diagram of the two systems is shown in Fig. 1.

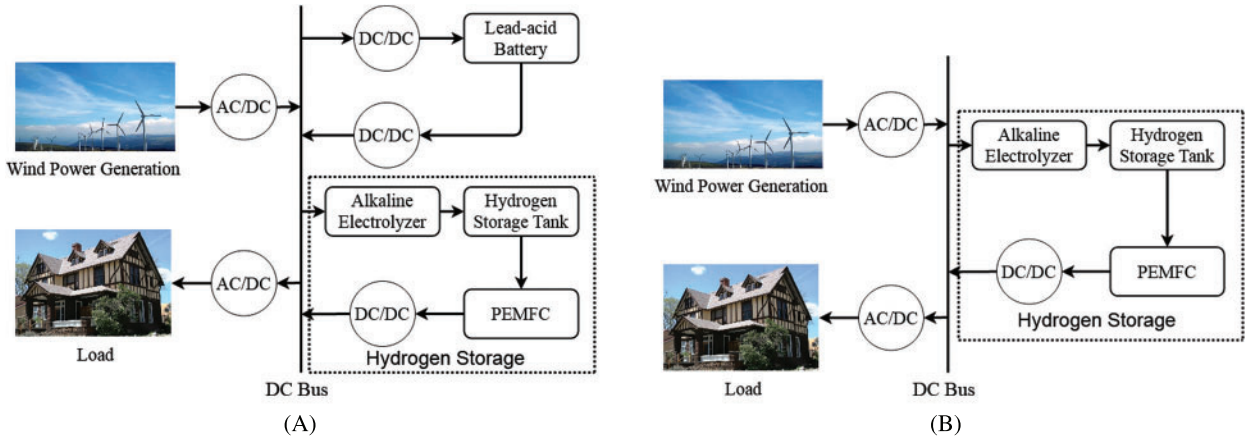

Figure 1: (A) System-I (B) System-II

The whole system consists of three parts: power generation, power storage and power consumption. In this paper, wind energy is the source of power generation. In the System I, lead-acid batteries work as energy storage to regulate and balance the load. After meeting the load demand, the excess power first enters the battery and then enters the electrolyzer. The function of the battery is to suppress fluctuations in the output power of wind power generation. However, the System I with the battery will reduce the capacity and cost of the hydrogen storage unit. Unlike the System I, the excess electricity generated in System II will directly enter the hydrogen storage unit. The power consumption in the load, divided into two types: DC load and AC load [31]. Considering the actual construction situation, DC bus and AC load have been used in the system.

2.2 Wind Turbine

The wind power generation system is mainly composed of a wind turbine and generator. The output power of a wind turbine is closely related to factors such as wind speed and blade material. In this study, we only considered the impact of wind speed on the output power of wind turbines. There are two parameters index defining wind speed, rated wind speed and boundary wind speed. The boundary wind speed mainly refers to the cut-in wind speed and the cut-out wind speed. When the actual wind speed is greater than the cut-in wind speed, the wind turbine begins running. The rated wind speed is between the cut-in wind speed and the cut-out wind speed, corresponding to the rated power. When the actual wind speed is greater than the rated wind speed but less than the cut-out wind speed, the wind turbine supplies energy with the rated power. To ensure the sunit's safety, the wind turbine will stop running when the actual wind speed

is greater than the cut-out wind speed. The mathematical model is shown in Eq. (1) [32].

$$P_W(t) = \begin{cases} 0 & v(t) < v_{in} \\ P_0 \times \dfrac{v(t) - v_{in}}{v_{rated} - v_{in}} & v_{in} \le v(t) \le v_{rated} \\ P_0 & v_{rated} \le v(t) \le v_{out} \\ 0 & v(t) > v_{out} \end{cases} \tag{1}$$

It is worth noting that the height of the wind measurement tower is usually different from that of the wind turbine hub. So, we need to use the power function method to simulate the vertical distribution of wind speed. It can be calculated by the Eq. (2) [33].

$$\frac{v_W}{v_H} = \left(\frac{H_W}{H_H}\right)^{\theta} \tag{2}$$

where θ is the coefficient of the wind speed energy law. It is affected by many factors such as altitude and season. In this study, we take the reference value 1/7, which under flat ground condition.

2.3 Lead-Acid Battery

The batteries are used in the system to improve the balance of power supply and demand. Its capacity is determined by the remaining power of the battery and the state of charge and discharge. The performance of the battery is evaluated by the instantaneous balance equation of the state of charge (SOC). The power of charging and discharging is shown in the Eqs. (3)–(4) [34].

$$P_{bat-c}(t) = P_{bat-in}(t) \times \eta_{bat-in} = \frac{dSOC}{dt} \tag{3}$$

$$-P_{bat-f}(t) = P_{bat-out}(t) \times \eta_{bat-out} = \frac{dSOC}{dt} \tag{4}$$

According to the working state of the battery, its mathematical model can be divided into four situations.

Case 1. The output power of the wind turbine is greater than the demand of the load, and the battery starts to charge. However, the capacity of the battery does not reach the maximum value of SOC. The state of charge of the battery at time t is as Eq. (5).

$$\begin{cases} SOC(t) = (1-\delta)SOC(t-1) + \dfrac{P_{bat-in}(t) \times \Delta t \times \eta_{bat-in}}{Q_0} \\ P_{bat-in}(t) = P_{ex} \end{cases} \tag{5}$$

Case 2. The output power of the wind turbine is greater than the demand of the load, and the battery starts to charge. The capacity of the battery has reached the maximum value of SOC.

However, there is still excess power. The state of charge of the battery at time t is as Eq. (6).

$$\begin{cases} SOC(t) = SOC_{\max} \\ P_{bat-in}(t) = \dfrac{[SOC_{\max} - SOC(t-1)] \times Q_0}{\Delta t} \end{cases} \tag{6}$$

Case 3. The output power of the wind turbine is lower than the demand of the load, and the battery starts to discharge. The capacity of the battery has not been reduced to the minimum value of SOC. The state of discharge of the battery at time t is as Eq. (7).

$$\begin{cases} SOC(t) = (1-\delta)SOC(t-1) - \dfrac{P_{bat-f}(t)\Delta t}{Q_0 \eta_{bat-out}} \\ P_{bat-f}(t) = P_{ex} \end{cases} \tag{7}$$

Case 4. The output power of the wind turbine is lower than the demand of the load, and the battery starts to discharge. The capacity of the battery has reduced to the minimum value of SOC. At this time, the batteries stop discharging. The state of discharge of the battery at time t is as Eq. (8).

$$\begin{cases} SOC(t) = SOC_{\min} \\ P_{bat-f}(t) = \dfrac{[SOC(t-1) - SOC_{\min}] \times Q_0}{\Delta t} \end{cases} \tag{8}$$

where η_{bat-in} is the charging efficiency of the battery; $\eta_{bat-out}$ is the discharge efficiency of the battery; δ is the self-discharge rate of the battery; Δt is the operating time of the battery.

2.4 Alkaline Electrolyzer

Hydrogen production by water electrolysis is a convenient way. The tank body filled with electrolyte is divided into anode suffocation and cathode suffocation by a diaphragm, and corresponding electrodes are placed in each chamber. At present, there are many studies on the application of acidic electrolyzer and alkaline electrolyzer in hybrid energy systems. Although the efficiency of an acidic electrolyzer is higher than that of an alkaline electrolyzer, its cost is higher. Therefore, the alkaline electrolyzer is used in the system proposed in this paper. The reaction equations of the anode and cathode are as follows [35]:

$$\begin{cases} 4OH^- \rightarrow O_2 + 2H_2O + 4e^- \\ 2H_2O + 4e^- \rightarrow O_2 + 4H^+ \end{cases} \Rightarrow 2H_2O \rightarrow O_2 + 2H_2 \tag{9}$$

According to Faraday's laws of electrolysis, the amount of gas produced by the electrolysis of water is proportional to the direct current. The mathematical model of the alkaline electrolyzer and hydrogen storage tank is as follows:

$$\begin{cases} P_{AE} = \dfrac{2Q_N N_A V_N}{3600 V_m C_0 \eta_{AE}} \\ Q = \dfrac{P_t Q_N}{P_{AE}} \\ N_{AE} = \dfrac{\max P_{net}}{P_{AE}} \end{cases} \tag{10}$$

where V_m is the molar volume of gas at room temperature and pressure; C_0 is the number of electrons per coulomb; P_t is the equivalent power of Q volume hydrogen.

For the hydrogen storage tank, we need to consider its actual hydrogen storage capacity. We ignored the influence of temperature on hydrogen storage.

$$N_{hst} = \frac{\max Q_{net}}{P_t}, \quad Q_{net} = \frac{Q_t P_{AE}}{r_0 C_0} \tag{11}$$

2.5 PEMFC

The fuel cell is based on hydrogen fuel and uses the principle of a redox reaction to convert the chemical energy in hydrogen fuel into electrical energy. PEMFC has the characteristics of low operating temperature, low noise and high power etc. It is suitable for hybrid energy systems. The PEMFC consists of cathode, anode and proton exchange membrane. The reaction equations of the anode and cathode is as follows [36]:

$$\begin{cases} 2H_2 \rightarrow 4H^+ + 4e^- \\ O_2 + 4H^+ + 4e^- \rightarrow 2H_2O \end{cases} \Rightarrow 2H_2 + O_2 \rightarrow 2H_2O \tag{12}$$

For the reaction process of PEMFC, the mathematical model can be expressed as the reverse process of electrolysis of water. We can use the Eq. (13).

$$P_{PEM} = \frac{2Q_{in} N_A V_N \eta_{PEM} \eta_t}{3600 V_m C_0} \tag{13}$$

3 Optimized Algorithm and Economic Modelling

In this section, we introduced the optimization algorithm, optimization objectives and constraints used in this research. The main optimization goal is the highest profit for the whole life cycle of the system. Besides, we also required that the loss of power supply probability does not exceed the maximum allowed.

3.1 The Non-Dominated Sorting Genetic Algorithm-II (NSGA-II)

For multi-objective optimization problems, genetic algorithm, particle swarm algorithm, NSGA-II, etc., are all applied. In a multi-objective optimization problem, multiple goals will influence each other. In other words, when the value of one target is increased, the other target may decrease. Therefore, we cannot achieve the optimal value of all the goals. NSGA-II was proposed by Kalyan-moy Deb in 2002. Unlike other algorithms, the NSGA-II provides a method to adjust the parameters between objects to achieve the best integration of the objective function. The calculation of NSGA-II can be roughly divided into three stages [33,37,38].

STAGE 1: The population is stratified according to the non-inferior solution level of the individual. Individuals at the same level have the same non-dominated order i0. Its purpose is to direct the search direction to the optimal Pareto solution set.

STAGE 2: NSGA-II adds individual crowded distance to it. Its purpose is to selectively sort individuals on the same level. In the calculation process, priority is given to selecting individuals with a crowded distance. This operation can make the calculation results evenly distributed in the target space, ensuring the diversity of the group.

STAGE 3: Keep the high-quality individuals in the parent directly into the offspring. Its purpose is to prevent the loss of the optimal solution that has been obtained.

Solving process of NSGA-II is shown in Fig. 2.

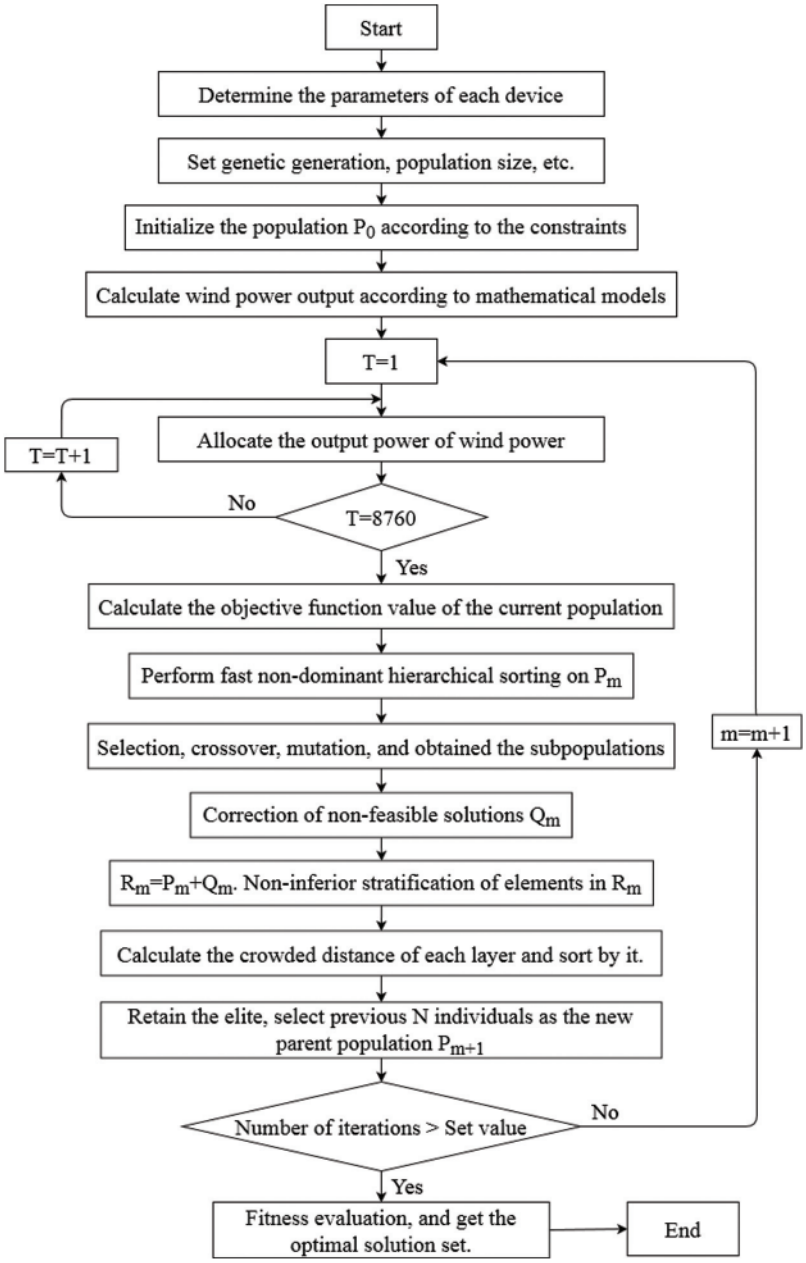

Figure 2: Solving process of NSGA-II

3.2 Optimization Goals and Constraints

3.2.1 Optimization Goals

In this paper, we considered the benefits of renewable energy generation to the environment and the time value of funds. The system economic model is established with the goal of profit maximization.

The cost of the system mainly includes the initial investment cost, replacement cost and maintenance cost. The income mainly includes hydrogen sales profit and environmental benefits. The subtraction of the two is the net profit of the system. The mathematical model is shown in the Eq. (14) [39].

$$\mathrm{MAX}R_{net} = \sum_{T=1}^{n} (R_{H_2,T} + R_{EN,T}) - C_0 \tag{14}$$

$$R_{H_2,T} = (Q_{AE,T} - Q_{FC,T}) \times S_{H_2} \tag{15}$$

$$R_{EN} = \sum_{X=1}^{n} [(\lambda_X + \mu_X) \times \Delta M_X] \tag{16}$$

$$C_0 = C_T \times \frac{i(1+i)^y}{(1+i)^y - 1} \tag{17}$$

$$C_T = \sum_{T=1}^{n} [(C_{CW} + C_{RW} + C_{MW})P_{W,T} + \underline{(C_{CB} + C_{RB} + C_{MB})P_{B,T}} + (C_{CA} + C_{RA} + C_{MA})P_{A,T} + (C_{CF} + C_{RF} + C_{MF})P_{F,T}] \tag{18}$$

Note: When calculating the cost of System-II, the underlined part should be deleted.

where λ_X is the environmental value of the Xth pollutant; μ_X is the penalty level of the Xth pollutant; ΔM_X is the annual reduction in emissions of type X pollutants caused by wind power generation; C_T is the cost of the life cycle of the system; C_{C*}, C_{R*}, C_{M*} is the initial construction cost of each component; subscript W, B, A, F is a wind turbine, lead-acid battery, alkaline electrolyzer and PEMFC; $P_{*,T}$ is the output power of each component at time T.

To optimize of wind-hydrogen hybrid energy storage systems operating in island mode, the loss of power supply probability (LPSP) is also an important optimization goal [40,41]. The load demand must be met first, and then profit maximization can be considered. The power reliability of the off-grid HWHE system is measured by the indicator of LPSP. To accurately show the operation of the system, this study used the time sequence method to characterize the LPSP. It is defined as the ratio of system power outage time to power supply time.

$$LPSP = \frac{\sum_{t=0}^{r} T\{[P_W(t) + P_{PEM}(t)] < P_L(t)\}}{T_t} \tag{19}$$

3.2.2 Constraints

The initial assumptions of the system configuration are based on the following constraints.

Considering the construction cost of wind farms, the scale of installed wind turbine capacity is determined according to load demand. The construction number of each piece of equipment should satisfy the Eq. (20).

$$\begin{cases} 0 < N_W < \dfrac{P}{P_0} \\ 0 < N_B < \dfrac{P}{P_{BN}} \\ 0 < N_F < \dfrac{P}{P_{FN}} \end{cases} \tag{20}$$

In the System I, the SOC of the battery at time t should not exceed the upper limit or fall below the lower limit [42]. Refer to the operating instructions of the lead-acid battery; we set up $SOC_{\max} = 0.8$, $SOC_{\min} = 0.2$.

$$SOC_{\min} \le SOC(t) \le SOC_{\max} \tag{21}$$

The LPSP should be lower than the maximum allowable value, which was set to 0.05 in this paper.

$$LPSP(t) \le LPSP_{\max} = 0.05 \tag{22}$$

The net hydrogen production at time T should be less than the volume of the hydrogen storage tank.

$$Q_{AE,T} - Q_{FC,T} \le Q_{\text{tank}} \tag{23}$$

4 Case Study

In order to verify the feasibility of the proposed method, the optimization scheme is realized by programming in MATLAB. Based on the above model analysis, the wind resource parameters in Ulanqab, Inner Mongolia Autonomous Region, China (N 42° 11′ 267″, E 112° 28′ 308″) in 2020 were selected as the calculation example. The wind speeds every 10 min is measured at a local height of 50 m. We used MATLAB to convert it to an hourly average (as shown in Fig. 3).

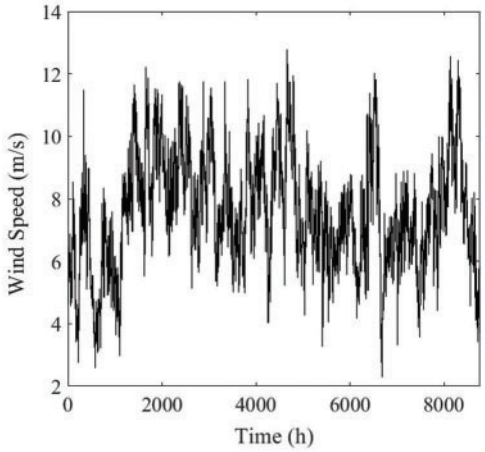

Figure 3: Hourly wind speed in 2020

We selected the hourly average load of the village in the study area for 24 h. Then we expanded the data for one day by 365 copies, and the load demand of 8760 h is shown in Fig. 4. It was worth noting that we ignored the real-time fluctuation of the load demand and only calculated the average value. Because real-time monitoring of load changes is beyond our scope of work. Moreover, this detail will not affect our results.

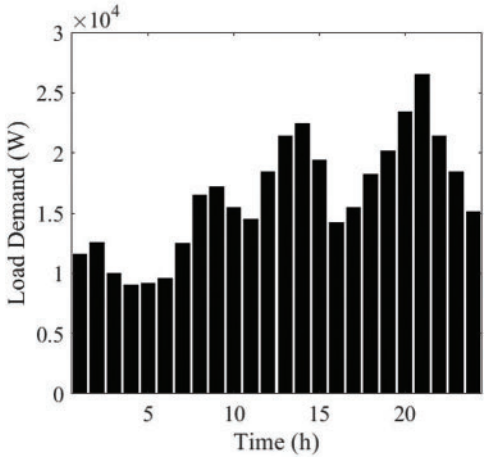

Figure 4: Average load demand per hour of one day

In this study, we chose FD-type wind turbines with a rated power of 10 kW. The rated wind speed is 10 m/s, the cut-in wind speed is 3 m/s, and the cut-out wind speed is 22 m/s. Chose a lead-acid battery with a rated capacity of 240 Ah and a rated voltage of 12 V. The parameters of the main components in the system are shown in Tab. 1. In terms of algorithm, the maximum number of iterations is set to 100. The initial population is 200. The crossover probability is 0.8. The mutation probability is 0.01.

Table 1: The economic parameters of each component in the system (Chinese yuan-CNY, ¥)

Components	Capacity	C_C/CNY	C_M/CNY	C_R/CNY	Life/year
Wind turbine	10000 W	76300	49500	0	20
Lead-acid battery	12 V·240 Ah	1500	3100	4900	5
Alkaline electrolyzer	8000 W	50880	9600	0	20
PEMFC	6000 W	18900	8280	0	20

To avoid the contingency of results caused by using a single algorithm. This study used GA and ant colony optimization (ACO), which frequently appear in multi-objective optimization problems. Moreover, we compared the calculation results of three algorithms. We have selected three groups among the many solutions of each algorithm, and got the final optimization result. The optimization results are shown in Tab. 2.

The SOC of the battery will affect its working life, thereby reducing the net profit of the system. The SOC of the lead-acid batteries for 8760 h throughout the year is shown in Fig. 5.

Table 2: The optimization results of NSGA-II, GA and ACO

Algorithm	Type	N_W	N_B	N_{AE}	N_F	LPSP	R_{net}/CNY	Optimal result
NSGA-II	System-I	2	96	1	1	0.01574	49,613	
		3	79	1	1	0.01941	42,241	
		3	61	1	2	0.01254	44,315	√
	System-II	2	0	2	3	0.03640	61,231	
		2	0	3	3	0.03244	58,663	√
		3	0	4	3	0.02281	41,024	
GA	System-I	3	106	1	2	0.01846	39,858	
		2	99	1	1	0.02151	42,509	
		2	85	1	2	0.01547	38,330	√
	System-II	2	0	2	4	0.03147	50,214	
		3	0	2	3	0.02816	48,190	√
		3	0	3	4	0.02140	39,474	
ACO	System-I	3	98	2	1	0.01744	43,110	
		3	139	1	1	0.01564	39,912	√
		2	108	1	2	0.01399	36,100	
	System-II	3	0	2	3	0.02441	46,320	
		2	0	3	3	0.03315	50,147	√
		2	0	3	4	0.02915	43,228	

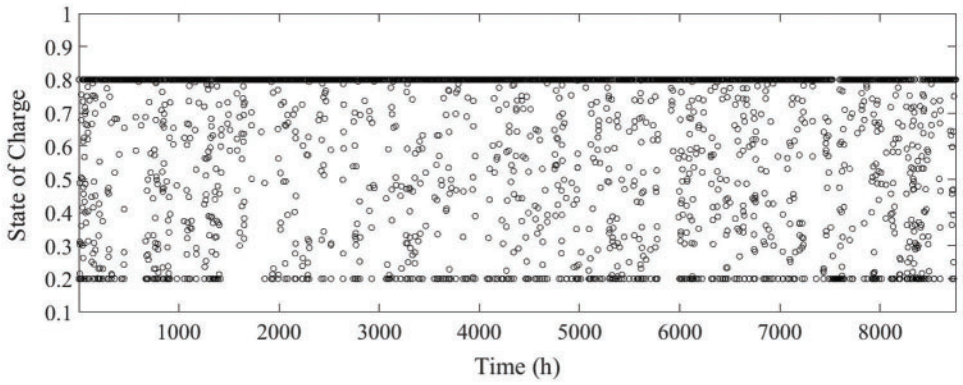

Figure 5: SOC of a lead-acid battery in 8760 h (NSGA-II)

In the whole year of 8760 h, the SOC of lead-acid battery fluctuates between 0.2–0.8, which is safe. This can protect the battery to the utmost extent and avoid the increase in system cost caused by frequent battery replacement. In addition, SOC has a relatively long time in 0.8. This means that the battery is in a sufficient state for a long time, guaranteeing the load demand to the greatest extent.

The iterative process curves of the three algorithms are shown in Fig. 6.

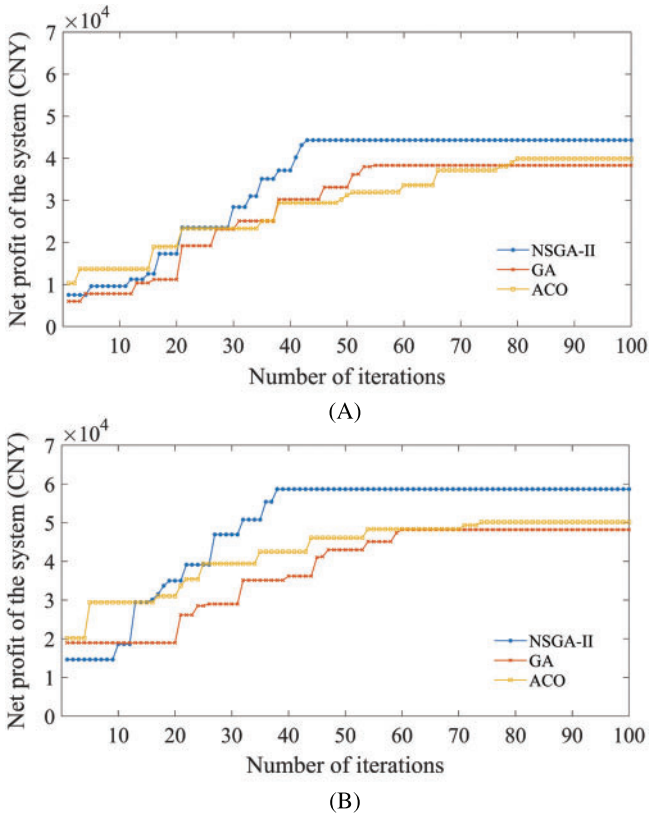

Figure 6: Iteration process curve of NSGA-II GA and ACO. (A) System-I (B) System-II

We can get the optimal configuration of the HWHE system by comparing the above optimization results. This study used three algorithms to compare the two systems. However, the calculation results showed that each has its advantages and disadvantages. So we need to discuss this deeply. In terms of algorithms, the calculation speed of NSGA-II is significantly better than GA and ACO. In the optimization process of System-I, NSGA-II converges in about 43 steps, while GA and ACO require 55 and 80 steps, respectively. In the optimization process of System-II, NSGA-II converges at about 38 steps, while GA and ACO require 60 and 74 steps, respectively. In terms of calculation results, the final profit of NSGA-II is higher than that of GA and ACO. The optimization result of NSGA-II for System-I is ¥44,315, which is 15.61% and 11.03% higher than GA and ACO, respectively. NSGA-II's optimization result for System-II is ¥58,663, which is 21.73% and 16.98% higher than GA and ACO, respectively.

By comparing the optimization results of the three algorithms, we found that the profit of System-II is higher than that of System-I. However, it is worth noting that the LPSP of System-I is generally lower than that of System-II. In other words, System-I is more reliable than System-II. In summary, NSGA-II has more advantages in optimization depth, optimization speed, and solution stability in optimizing the HWHE system. As for the choice of the system, System-II has higher profits, but its reliability has deteriorated, while System-I is the opposite. Therefore, the research personnel should fully consider the joint influence of net profit and LPSP in selecting the system. The required architecture for the System-I composes of 3 numbers of 10 kW wind turbines, 61 sets of 12 V·240 Ah lead-acid batteries, 8 kW electrolytic cell, and 6 kW PEMFC.

The net profit and LPSP are ¥44,315 and 0.01254, respectively. The required architecture for the System-II composes of 2 numbers of 10 kW wind turbines, 24 kW electrolytic cells, and 18 kW PEMFC. Net profit and LPSP are ¥58,663 and 0.03244, respectively.

5 Conclusion

Wind energy is one of the renewable energy sources which has been widely used. However, the uncertainty of its power generation and the nonlinearity of load demand make it very complicated to determine the capacity of each device in the hybrid renewable energy power generation system. HWHE system has advantages in compared with independent wind power generation systems. This paper took the area of Northwest China as an example and proposed two kinds of HWHE systems. In the absence of grid power, the hybrid system supplies power to the area. Firstly, we established steady-state models of the wind turbine, alkaline electrolyzer, lead-acid battery and PEMFC in MATLAB to optimize the capacity. Secondly, we analyzed the operating mode of the system and determined two system structures (the system contains batteries whether or not). Finally, we compared the economics of the two systems and selected the optimal configuration for the area according to the wind speed and load in the sample area. In the same calculation example data, the non-dominated sorting genetic algorithm-II, genetic algorithm and ant colony optimization is used to optimize the capacity of each device in the two systems. As a result, NSGA-II's optimization result for System-II is 21.73% and 16.98% higher than GA and ACO, respectively. The optimization result of NSGA-II for System-I is 15.61% and 11.03% higher than GA and ACO, respectively. Besides, the cost of a battery-equipped system is 32.38% higher than another system by NSGA-II. As for the choice of the system, System-II has higher profits, but its reliability has deteriorated, while System-I is the opposite. Therefore, the research personnel should fully consider the joint influence of net profit and LPSP in selecting the system. This article provided the theoretical basis and data support for decision-makers to design HWHE system. And also promoted the development and construction of off-grid integrated energy systems.

Acknowledgement: We would like to thank all those who have reviewed and contributed to this paper for their valuable assistance.

Funding Statement: This work was supported by the Inner Mongolia Science and Technology Program under Grant 2021GG0336, and by the Open Fund of Key Laboratory of Wind Energy and Solar Energy Technology (Inner Mongolia University of Technology), Ministry of Education (No. 2020ZD01) in China.

Conflicts of Interest: The authors declare that they have no conflicts of interest to report regarding the present study.

References

1. Dyer, J. A., Desjardins, R. L. (2009). A review and evaluation of fossil energy and carbon dioxide emissions in Canadian agriculture. *Journal of Sustainable Agriculture, 33(2),* 210–228. DOI 10.1080/10440040802660137.
2. Ediger, V. S. (2019). An integrated review and analysis of multi-energy transition from fossil fuels to renewables. *5th International Conference on Power and Energy Systems Engineering*, vol. 156, pp. 2–6. Nagoya, Japan. DOI 10.1016/j.egypro.2018.11.073.

3. Acar, C., Dincer, I. (2019). Review and evaluation of hydrogen production options for better environment. *Journal of Cleaner Production, 218,* 835–849. DOI 10.1016/j.jclepro.2019.02.046.
4. Su, C. G., Cheng, C. T., Wang, P. L., Shen, J. J., Wu, X. Y. (2019). Optimization model for long-distance integrated transmission of wind farms and pumped-storage hydropower plants. *Applied Energy, 242,* 285–293. DOI 10.1016/j.apenergy.2019.03.080.
5. Samy, M. M., Mosaad, M. I., El-Naggar, M. F., Barakat, S. (2021). Reliability support of undependable grid using green energy systems: Economic study. *IEEE Access, 9,* 14528–14539. DOI 10.1109/ACCESS.2020.3048487.
6. Malik, M. Z., Baloch, M. H., Gul, M., Kaloi, G. S., Chauhdary, S. T. et al. (2021). A research on conventional and modern algorithms for maximum power extraction from wind energy conversion system: A review. *Environmental Science and Pollution Research, 28(5),* 5020–5035. DOI 10.1007/s11356-020-11558-6.
7. Ayodele, T. R., Mosetlhe, T. C., Yusuff, A. A., Ogunjuyigbe, A. S. O. (2021). Off-grid hybrid renewable energy system with hydrogen storage for South African rural community health clinic. *International Journal of Hydrogen Energy, 46(38),* 19871–19885. DOI 10.1016/j.ijhydene.2021.03.140.
8. Bagherian, M. A., Mehranzamir, K. (2020). A comprehensive review on renewable energy integration for combined heat and power production. *Energy Conversion and Management, 224,* 113454. DOI 10.1016/j.enconman.2020.113454.
9. Tazay, A. F., Samy, M. M., Barakat, S. (2020). A techno-economic feasibility analysis of an autonomous hybrid renewable energy sources for university building at Saudi Arabia. *Journal of Electrical Engineering & Technology, 15(6),* 2519–2527. DOI 10.1007/s42835-020-00539-x.
10. Zhang, Y. M., Wang, L. G., Wang, N. L., Duan, L. Q., Zong, Y. et al. (2019). Balancing wind-power fluctuation via onsite storage under uncertainty: Power-to-hydrogen-to-power versus lithium battery. *Renewable & Sustainable Energy Reviews, 116,* 109465. DOI 10.1016/j.rser.2019.109465.
11. Gokcek, M., Kale, C. (2018). Optimal design of a hydrogen refuelling station (HRFS) powered by hybrid power system. *Energy Conversion and Management, 161,* 215–224. DOI 10.1016/j.enconman.2018.02.007.
12. Dutta, S. (2014). A review on production, storage of hydrogen and its utilization as an energy resource. *Journal of Industrial and Engineering Chemistry, 20(4),* 1148–1156. DOI 10.1016/j.jiec.2013.07.037.
13. Hosseini, S. E., Wahid, M. A. (2016). Hydrogen production from renewable and sustainable energy resources: Promising green energy carrier for clean development. *Renewable & Sustainable Energy Reviews, 57,* 850–866. DOI 10.1016/j.rser.2015.12.112.
14. Bukar, A. L., Tan, C. W. (2019). A review on stand-alone photovoltaic-wind energy system with fuel cell: System optimization and energy management strategy. *Journal of Cleaner Production, 221,* 73–88. DOI 10.1016/j.jclepro.2019.02.228.
15. Roy, P., He, J. B., Liao, Y. (2020). Cost minimization of battery-supercapacitor hybrid energy storage for hourly dispatching wind-solar hybrid power system. *IEEE Access, 8,* 210099–210115. DOI 10.1109/ACCESS.2020.3037149.
16. Wu, K. H., Zhou, H., Liu, J. Z. (2014). Optimal capacity allocation of large-scale wind-PV-battery units. *International Journal of Photoenergy, 2014,* 539414. DOI 10.1155/2014/539414.
17. Chen, H. C. (2013). Optimum capacity determination of stand-alone hybrid generation system considering cost and reliability. *Applied Energy, 103,* 155–164. DOI 10.1016/j.apenergy.2012.09.022.
18. Ma, T., Yang, H. X., Lu, L. (2014). A feasibility study of a stand-alone hybrid solar-wind-battery system for a remote island. *Applied Energy, 121,* 149–158. DOI 10.1016/j.apenergy.2014.01.090.
19. Yimen, N., Tchotang, T., Kanmogne, A., Idriss, I. A., Musa, B. et al. (2020). Optimal sizing and techno-economic analysis of hybrid renewable energy systems–A case study of a photovoltaic/wind/battery/diesel system in Fanisau, Northern Nigeria. *Processes, 8(11),* 1381. DOI 10.3390/pr8111381.
20. Li, J. Z., Liu, P., Li, Z. (2020). Optimal design and techno-economic analysis of a solar-wind-biomass off-grid hybrid power system for remote rural electrification: A case study of west China. *Energy, 208,* 118387. DOI 10.1016/j.energy.2020.118387.

21. Samy, M. M., Barakat, S., Ramadan, H. S. (2019). A flower pollination optimization algorithm for an off-grid PV-fuel cell hybrid renewable system. *International Journal of Hydrogen Energy, 44(4),* 2141–2152. DOI 10.1016/j.ijhydene.2018.05.127.
22. Rabaia, M. K. H., Abdelkareem, M. A., Sayed, E. T., Elsaid, K., Chae, K. J. et al. (2021). Environmental impacts of solar energy systems: A review. *Science of the Total Environment, 754,* 141989. DOI 10.1016/j.scitotenv.2020.141989.
23. Khan, F. A., Pal, N., Saeed, S. H. (2018). Review of solar photovoltaic and wind hybrid energy systems for sizing strategies optimization techniques and cost analysis methodologies. *Renewable & Sustainable Energy Reviews, 92,* 937–947. DOI 10.1016/j.rser.2018.04.107.
24. Kasprzyk, L., Tomczewski, A., Pietracho, R., Mielcarek, A., Nadolny, Z. et al. (2020). Optimization of a PV-wind hybrid power supply structure with electrochemical storage intended for supplying a load with known characteristics. *Energies, 13(22),* 6143. DOI 10.3390/en13226143.
25. Eteiba, M. B., Barakat, S., Samy, M. M., Wahba, W. I. (2018). Optimization of an off-grid PV/Biomass hybrid system with different battery technologies. *Sustainable Cities and Society, 40,* 713–727. DOI 10.1016/j.scs.2018.01.012.
26. Chen, X. P., Cao, W. P., Xing, L. (2019). GA optimization method for a multi-vector energy system incorporating wind, hydrogen, and fuel cells for rural village applications. *Applied Sciences-Basel, 9(17),* 3554. DOI 10.3390/app9173554.
27. Wang, Z. K., Jia, Y., Cai, C., Chen, Y. P., Li, N. et al. (2021). Study on the optimal configuration of a wind-solar-battery-fuel cell system based on a regional power supply. *IEEE Access, 9,* 47056–47068. DOI 10.1109/ACCESS.2021.3064888.
28. Kasseris, E., Samaras, Z., Zafeiris, D. (2007). Optimization of a wind-power fuel-cell hybrid system in an autonomous electrical network environment. *Renewable Energy, 32(1),* 57–79. DOI 10.1016/j.renene.2005.12.011.
29. Rakipour, D., Barati, H. (2019). Probabilistic optimization in operation of energy hub with participation of renewable energy resources and demand response. *Energy, 173,* 384–399. DOI 10.1016/j.energy.2019.02.021.
30. Rosales-Asensio, E., Rosales, A. E., Colmenar-Santos, A. (2021). Y surrogate optimization of coupled energy sources in a desalination microgrid based on solar PV and wind energy. *Desalination, 500,* 114882. DOI 10.1016/j.desal.2020.114882.
31. Jahangiri, M., Soulouknga, M. H., Bardei, F. K., Shamsabadi, A. A., Akinlabi, E. T. et al. (2019). Techno-econo-environmental optimal operation of grid-wind-solar electricity generation with hydrogen storage system for domestic scale, case study in Chad. *International Journal of Hydrogen Energy, 44(54),* 28613–28628. DOI 10.1016/j.ijhydene.2019.09.130.
32. Fang, R. M. (2019). Life cycle cost assessment of wind power-hydrogen coupled integrated energy system. *International Journal of Hydrogen Energy, 44(56),* 29399–29408. DOI 10.1016/j.ijhydene.2019.03.192.
33. Xu, C. B., Ke, Y. M., Li, Y. B., Chu, H., Wu, Y. N. (2020). Data-driven configuration optimization of an off-grid wind/PV/hydrogen system based on modified NSGA-II and CRITIC-TOPSIS. *Energy Conversion and Management, 215,* 112892. DOI 10.1016/j.enconman.2020.112892.
34. Alturki, F. A., Farh, H. M. H., Al-Shamma'a, A. A., AlSharabi, K. (2020). Techno-economic optimization of small-scale hybrid energy systems using manta ray foraging optimizer. *Electronics, 9(12),* 2045. DOI 10.3390/electronics9122045.
35. Ulleberg, O. (2003). Modeling of advanced alkaline electrolyzers: A system simulation approach. *International Journal of Hydrogen Energy, 28(1),* 21–33. DOI 10.1016/S0360-3199(02)00033-2.
36. Fang, W. H., Guo, Y. F., Wang, F. C. (2015). The development and power management of a stationary pemfc hybrid power system. *8th IEEE/SICE International Symposium on System Integration,* pp. 684–689. Meijo University, Nagoya, Japan, IEEE.
37. Aghbashlo, M., Hosseinpour, S., Tabatabaei, M., Younesi, H., Najafpour, G. (2016). On the exergetic optimization of continuous photobiological hydrogen production using hybrid ANFIS-nSGA-II (adaptive neuro-fuzzy inference system-non-dominated sorting genetic algorithm-II). *Energy, 96,* 507–520. DOI 10.1016/j.energy.2015.12.084.

38. Kamjoo, A., Maheri, A., Dizqah, A. M., Putrus, G. A. (2016). Multi-objective design under uncertainties of hybrid renewable energy system using NSGA-II and chance constrained programming. *International Journal of Electrical Power & Energy Systems, 74,* 187–194. DOI 10.1016/j.ijepes.2015.07.007.
39. Bornapour, M., Hooshmand, R. A., Parastegari, M. (2019). An efficient scenario-based stochastic programming method for optimal scheduling of CHP-pEMFC, WT, PV and hydrogen storage units in micro grids. *Renewable Energy, 130,* 1049–1066. DOI 10.1016/j.renene.2018.06.113.
40. Alturki, F. A., Al-Shamma'a, A. A., Farh, H. M. H., AlSharabi, K. (2021). Optimal sizing of autonomous hybrid energy system using supply-demand-based optimization algorithm. *International Journal of Energy Research, 45(1),* 605–625. DOI 10.1002/er.5766.
41. Anoune, K., Ghazi, M., Bouya, M., Laknizi, A., Ghazouani, M. et al. (2020). Optimization and techno-economic analysis of photovoltaic-wind-battery based hybrid system. *Journal of Energy Storage, 32,* 101878. DOI 10.1016/j.est.2020.101878.
42. Subramanian, S., Sankaralingam, C., Elavarasan, R. M., Vijayaraghavan, R. R., Raju, K. et al. (2021). An evaluation on wind energy potential using multi-objective optimization based non-dominated sorting genetic algorithm III. *Sustainability, 13(1),* 410. DOI 10.3390/su13010410.